

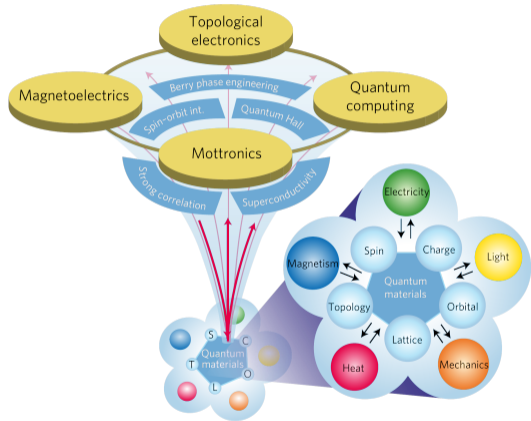
International Summer School on Computational Quantum Materials 2024

Ab initio description of strongly correlated materials: combining density functional theory plus and dynamical mean-field theory

Sophie Beck

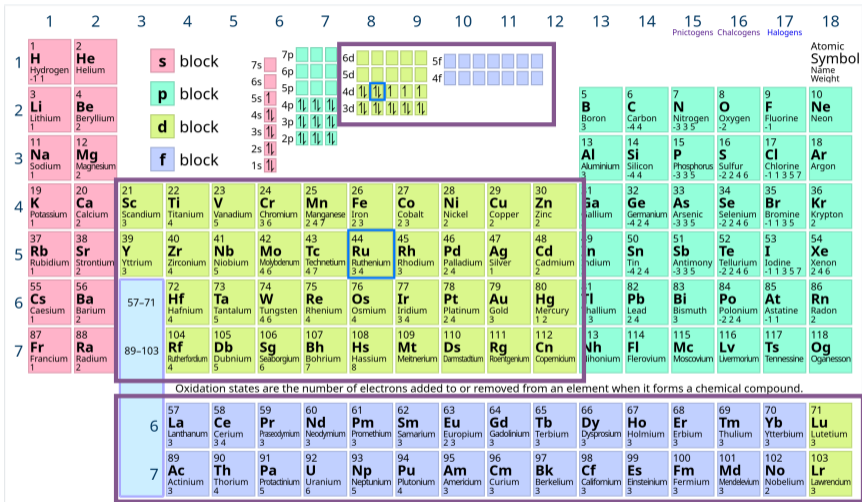
27th May 2024





- sensitive to small changes in external parameters:
 - temperature
 - pressure
 - doping
 - ...
- emerging phenomena:
 - high T_C superconductivity
 - colossal magnetoresistance
 - Mott physics
 - ...

Correlated d -/ f -shells

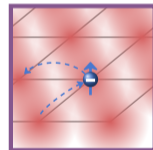
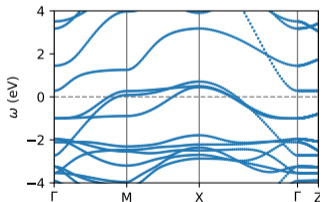


Weak versus strong correlation

weakly correlated systems

- effective single-particle picture
- density functional theory

$$\begin{aligned} \Psi(\mathbf{x}_1, \mathbf{x}_2) &= \frac{1}{\sqrt{2}} \{ \chi_1(\mathbf{x}_1)\chi_2(\mathbf{x}_2) - \chi_1(\mathbf{x}_2)\chi_2(\mathbf{x}_1) \} \\ &= \frac{1}{\sqrt{2}} \begin{vmatrix} \chi_1(\mathbf{x}_1) & \chi_2(\mathbf{x}_1) \\ \chi_1(\mathbf{x}_2) & \chi_2(\mathbf{x}_2) \end{vmatrix}, \end{aligned}$$



Weak versus strong correlation

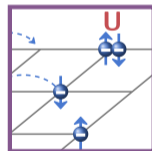
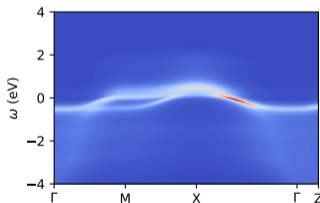
weakly correlated systems

- effective single-particle picture
- density functional theory

strongly correlated systems

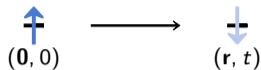
- breakdown of single-particle picture
- large local Coulomb interaction U
- between ionic localization and itinerant behavior

$$\begin{aligned} \Psi(\mathbf{x}_1, \mathbf{x}_2) &= \frac{1}{\sqrt{2}} \{ \chi_1(\mathbf{x}_1)\chi_2(\mathbf{x}_2) - \chi_1(\mathbf{x}_2)\chi_2(\mathbf{x}_1) \} \\ &= \frac{1}{\sqrt{2}} \begin{vmatrix} \chi_1(\mathbf{x}_1) & \chi_2(\mathbf{x}_1) \\ \chi_1(\mathbf{x}_2) & \chi_2(\mathbf{x}_2) \end{vmatrix}, \end{aligned}$$



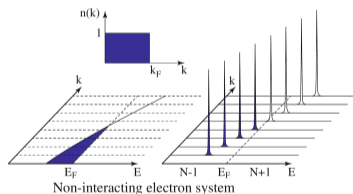
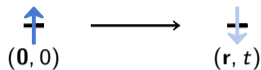
Spectral function $A(\mathbf{k}, \omega)$

$$A(\mathbf{k}, \omega) = \frac{1}{\pi} \text{Im} \int d\mathbf{r} \int dt e^{i(\mathbf{k}\mathbf{r} - \omega t)} \underbrace{i\theta(t) \langle [\Psi(\mathbf{r}, t), \Psi^\dagger(\mathbf{0}, 0)] \rangle}_{G^R(\mathbf{r}, t)}$$



Spectral function $A(\mathbf{k}, \omega)$ - non-interacting

$$A(\mathbf{k}, \omega) = \frac{1}{\pi} \text{Im} \int d\mathbf{r} \int dt e^{i(\mathbf{k}\mathbf{r} - \omega t)} \underbrace{i\theta(t) \langle [\Psi(\mathbf{r}, t), \Psi^\dagger(\mathbf{0}, 0)] \rangle}_{G^R(\mathbf{r}, t)}$$

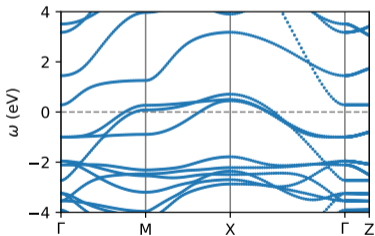
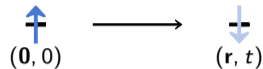


$$G(\mathbf{k}, \omega) = \frac{1}{\omega - \epsilon_{\mathbf{k}} + i\eta}$$

$$A(\mathbf{k}, \omega) = -\frac{1}{\pi} \delta(\omega - \epsilon_{\mathbf{k}})$$

Spectral function $A(\mathbf{k}, \omega)$ - non-interacting

$$A(\mathbf{k}, \omega) = \frac{1}{\pi} \text{Im} \int d\mathbf{r} \int dt e^{i(\mathbf{k}\mathbf{r} - \omega t)} \underbrace{i\theta(t) \langle [\Psi(\mathbf{r}, t), \Psi^\dagger(\mathbf{0}, 0)] \rangle}_{G^R(\mathbf{r}, t)}$$



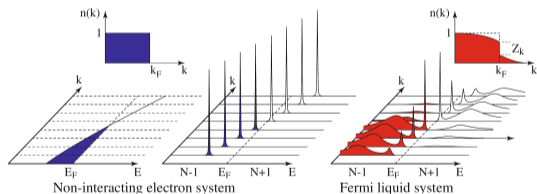
$$G(\mathbf{k}, \omega) = \frac{1}{\omega - \epsilon_{\mathbf{k}} + i\eta}$$

$$A(\mathbf{k}, \omega) = -\frac{1}{\pi} \delta(\omega - \epsilon_{\mathbf{k}})$$

Spectral function $A(\mathbf{k}, \omega)$ - interacting

$$A(\mathbf{k}, \omega) = \frac{1}{\pi} \text{Im} \int d\mathbf{r} \int dt e^{i(\mathbf{k}\mathbf{r} - \omega t)} \underbrace{i\theta(t) \langle [\Psi(\mathbf{r}, t), \Psi^\dagger(\mathbf{0}, 0)] \rangle}_{G^R(\mathbf{r}, t)}$$

$$\begin{array}{ccc} \uparrow & \longrightarrow & \downarrow \\ (0, 0) & & (\mathbf{r}, t) \end{array}$$



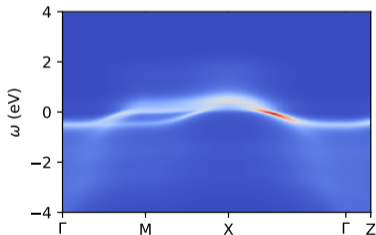
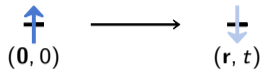
$$G(\mathbf{k}, \omega) = \frac{1}{\omega - \epsilon_{\mathbf{k}} - \Sigma(\omega)}$$

$$\Sigma(\omega) = \Sigma'(\omega) + i\Sigma''(\omega)$$

$$A(\mathbf{k}, \omega) = -\frac{1}{\pi} \frac{\Sigma''(\omega)}{(\omega - \epsilon_{\mathbf{k}} - \Sigma'(\omega))^2 + \Sigma''(\omega)^2}$$

Spectral function $A(\mathbf{k}, \omega)$ - interacting

$$A(\mathbf{k}, \omega) = \frac{1}{\pi} \text{Im} \int d\mathbf{r} \int dt e^{i(\mathbf{k}\mathbf{r} - \omega t)} \underbrace{i\theta(t) \langle [\Psi(\mathbf{r}, t), \Psi^\dagger(\mathbf{0}, 0)] \rangle}_{G^R(\mathbf{r}, t)}$$

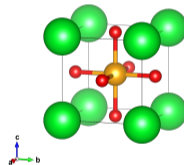
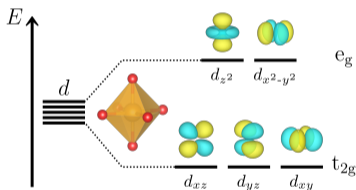
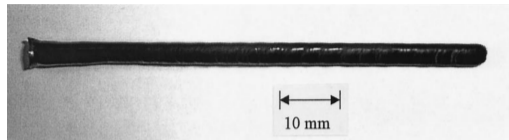
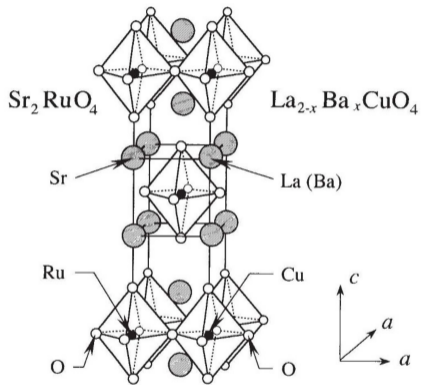


$$G(\mathbf{k}, \omega) = \frac{1}{\omega - \epsilon_{\mathbf{k}} - \Sigma(\omega)}$$

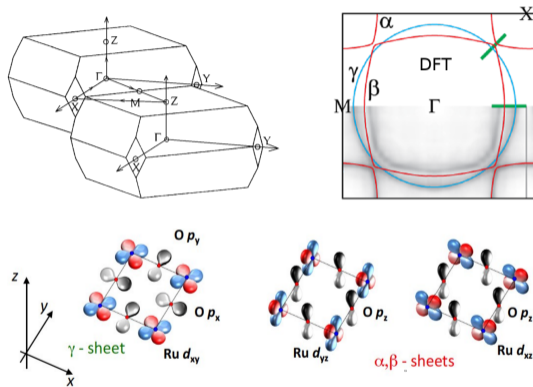
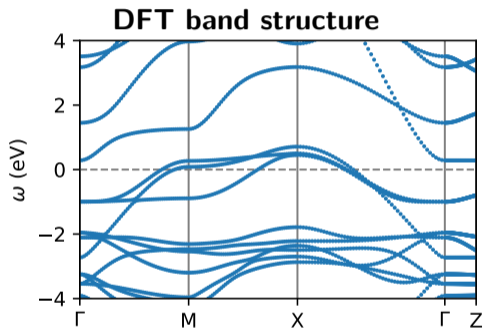
$$\Sigma(\omega) = \Sigma'(\omega) + i\Sigma''(\omega)$$

$$A(\mathbf{k}, \omega) = -\frac{1}{\pi} \frac{\Sigma''(\omega)}{(\omega - \epsilon_{\mathbf{k}} - \Sigma'(\omega))^2 + \Sigma''(\omega)^2}$$

Case study: Fermi surface of Sr_2RuO_4



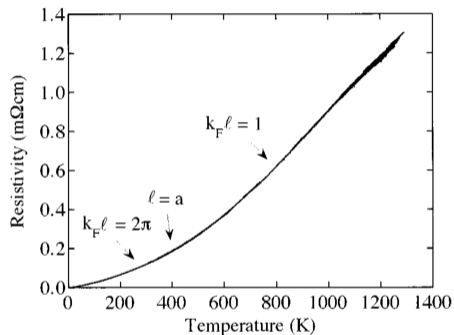
- octahedral crystal field
- key action in t_{2g} subspace



M. W. Haverkort *et al.*, Phys. Rev. Lett. 101, 026406 (2008)

The electronic structure of Sr_2RuO_4

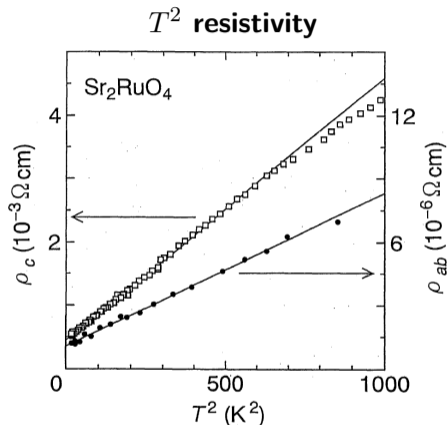
- correlated metal ($U = 2.3$ eV)



A. W. Tyler *et al.*, Phys. Rev. B 58, R10107 (1998)

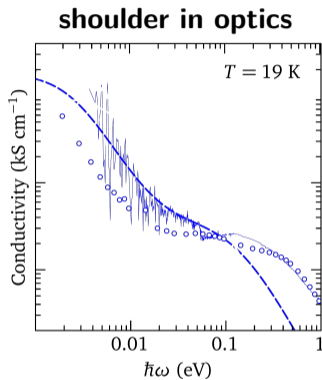
The electronic structure of Sr_2RuO_4

- correlated metal ($U = 2.3$ eV)
- Fermi liquid ($T_{\text{FL}} \approx 25$ K)



Y. Maeno *et al.*, J. Phys. Soc. Jpn. 66, 1405 (1997)

- correlated metal ($U = 2.3$ eV)
- Fermi liquid ($T_{\text{FL}} \approx 25$ K)

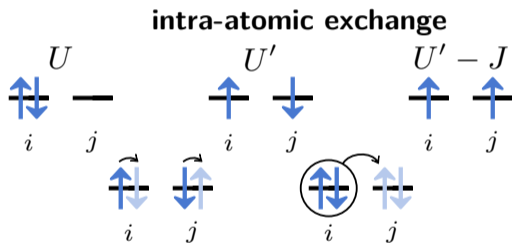


D. Stricker *et al.*, Phys. Rev. Lett. 113, 087404 (2014)

- self-energy $\Sigma''(\omega, T) \sim \omega^2 + (\pi T)^2$

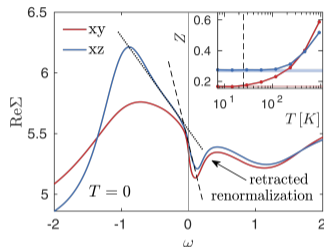
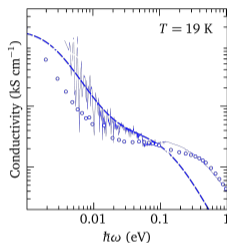
The electronic structure of Sr_2RuO_4

- correlated metal ($U = 2.3$ eV)
- Fermi liquid ($T_{\text{FL}} \approx 25$ K)
- Hund physics ($J = 0.4$ eV)



- correlated metal ($U = 2.3$ eV)
- Fermi liquid ($T_{\text{FL}} \approx 25$ K)
- Hund physics ($J = 0.4$ eV)

two-stage coherence, orbital differentiation

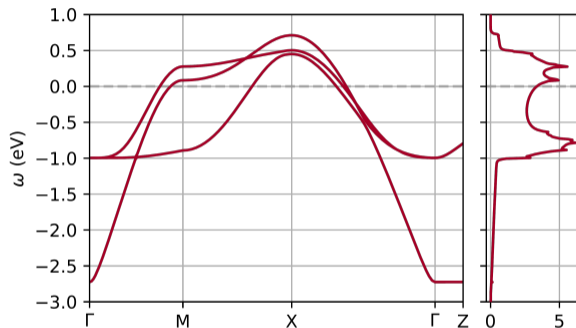


F. Kugler *et al.*, Phys. Rev. Lett. 124, 016401 (2020)

- non-FL excess of spectral weight
- e.g. quantum oscillation, NMR spectroscopy, ...

The electronic structure of Sr_2RuO_4

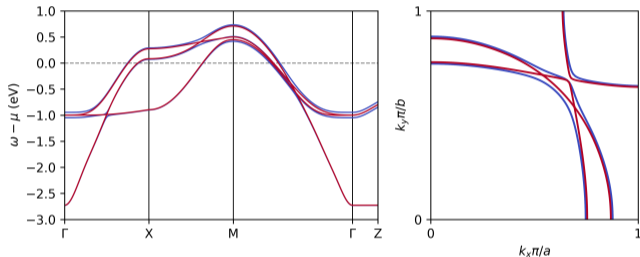
- correlated metal ($U = 2.3$ eV)
- Fermi liquid ($T_{\text{FL}} \approx 25$ K)
- Hund physics ($J = 0.4$ eV)
- Van Hove singularity close to E_{F}



- drives orbital differentiation

The electronic structure of Sr_2RuO_4

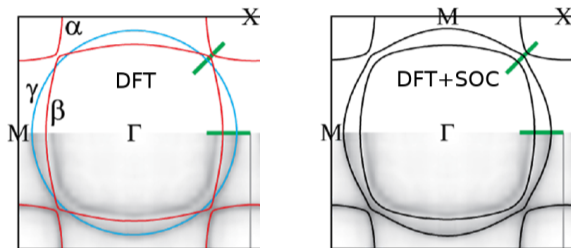
- correlated metal ($U = 2.3$ eV)
- Fermi liquid ($T_{\text{FL}} \approx 25$ K)
- Hund physics ($J = 0.4$ eV)
- Van Hove singularity close to E_{F}
- spin-orbit coupling ($\lambda \approx 0.2$ eV)



- strong effect of SOC on Fermi surface

The electronic structure of Sr_2RuO_4

- correlated metal ($U = 2.3$ eV)
- Fermi liquid ($T_{\text{FL}} \approx 25$ K)
- Hund physics ($J = 0.4$ eV)
- Van Hove singularity close to E_{F}
- spin-orbit coupling ($\lambda \approx 0.2$ eV)

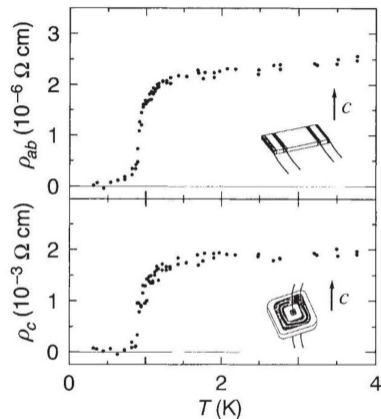


M. W. Haverkort *et al.*, Phys. Rev. Lett. 101, 026406 (2008)

- strong effect of SOC on Fermi surface

The electronic structure of Sr_2RuO_4

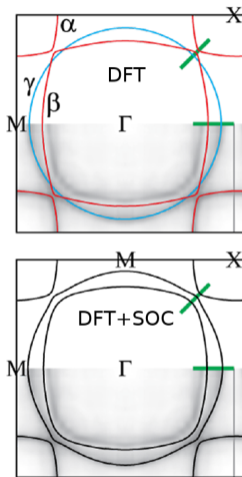
- correlated metal ($U = 2.3$ eV)
- Fermi liquid ($T_{\text{FL}} \approx 25$ K)
- Hund physics ($J = 0.4$ eV)
- Van Hove singularity close to E_{F}
- spin-orbit coupling ($\lambda \approx 0.2$ eV)
- superconductivity ($T_{\text{C}} \approx 1.5$ K)



Y. Maeno *et al.*, Nature 372, 532 (1994)

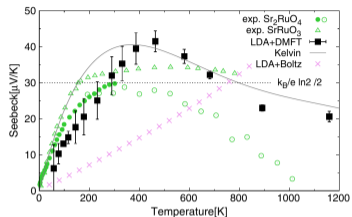
Where DFT may be insufficient

Fermi surface



M. W. Haverkort *et al.*, Phys. Rev. Lett. 101, 026406 (2008)

Seebeck



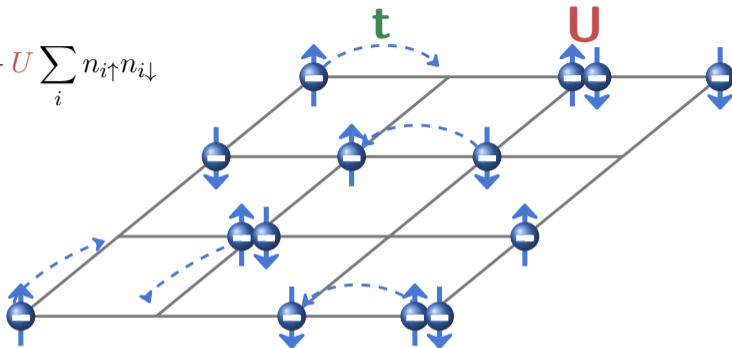
- also: mass enhancement, orbital occupations, optics, SOC, ...
- **more obvious**: local-moment paramagnet (**Mott insulator**) versus (anti-)ferromagnet or non-magnetic metal in DFT

J. Mravlje, A. Georges, Phys. Rev. Lett. 117, 036401 (2016)

- **situation:** complex physics arising from strong local Coulomb interaction in partially filled orbitals in strongly correlated materials
- **goal:** ab-initio, material-realistic description
- **challenge:** combining localized, atomic-like and itinerant electronic behavior
- **ansatz:** DFT+DMFT, downfolding & embedding
- **example:** Fermi surface of Sr_2RuO_4

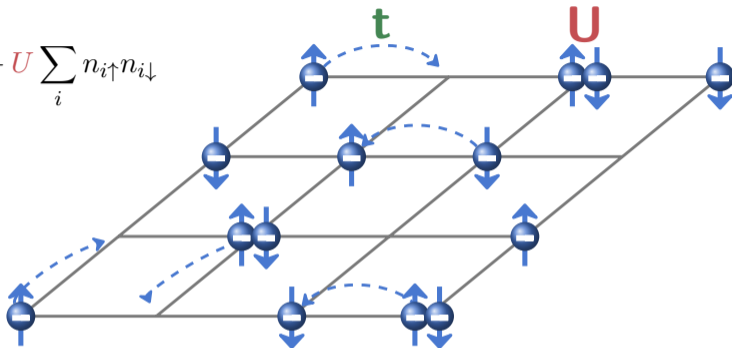
recap: the Hubbard model

$$H = - \sum_{ij, \sigma} t_{ij} c_{i\sigma}^\dagger c_{j\sigma} + U \sum_i n_{i\uparrow} n_{i\downarrow}$$

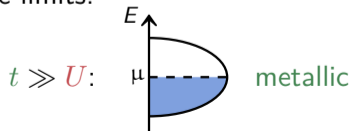


recap: the Hubbard model

$$H = - \sum_{ij, \sigma} t_{ij} c_{i\sigma}^\dagger c_{j\sigma} + U \sum_i n_{i\uparrow} n_{i\downarrow}$$

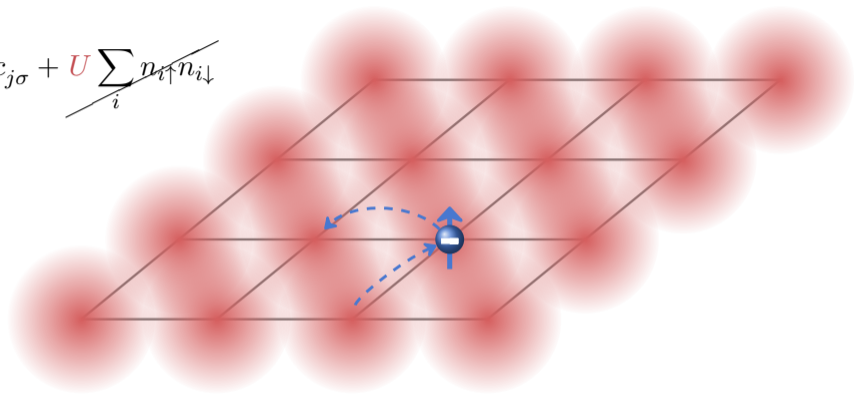


In the limits:

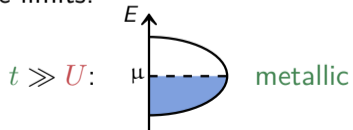


recap: the Hubbard model

$$H = - \sum_{ij, \sigma} t_{ij} c_{i\sigma}^\dagger c_{j\sigma} + U \sum_i n_{i\uparrow} n_{i\downarrow}$$

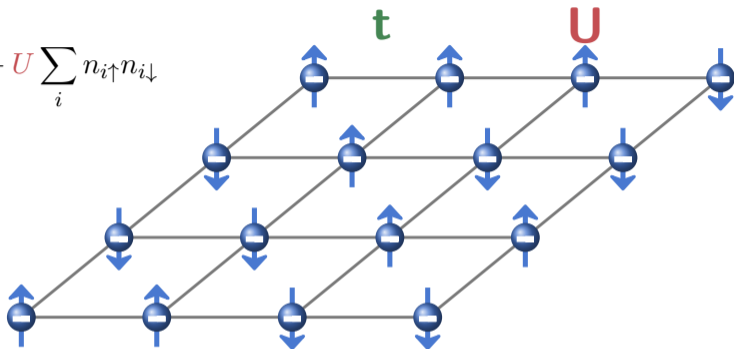


In the limits:

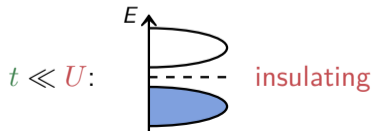
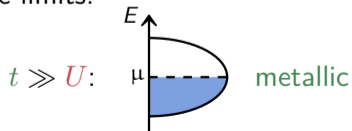


recap: the Hubbard model

$$H = - \sum_{ij,\sigma} t_{ij} c_{i\sigma}^\dagger c_{j\sigma} + U \sum_i n_{i\uparrow} n_{i\downarrow}$$

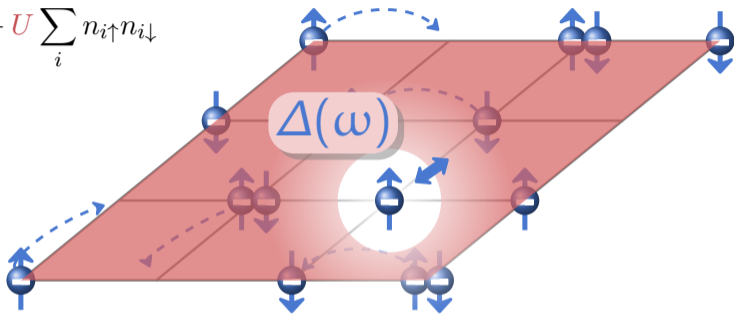


In the limits:



recap: Dynamical Mean Field Theory

$$H = - \sum_{ij, \sigma} t_{ij} c_{i\sigma}^\dagger c_{j\sigma} + U \sum_i n_{i\uparrow} n_{i\downarrow}$$



- map lattice to effective impurity model (AIM) embedded in bath
- impurity-bath coupling $\Delta(\omega)$ determined self-consistently
- basic ingredients: t, U

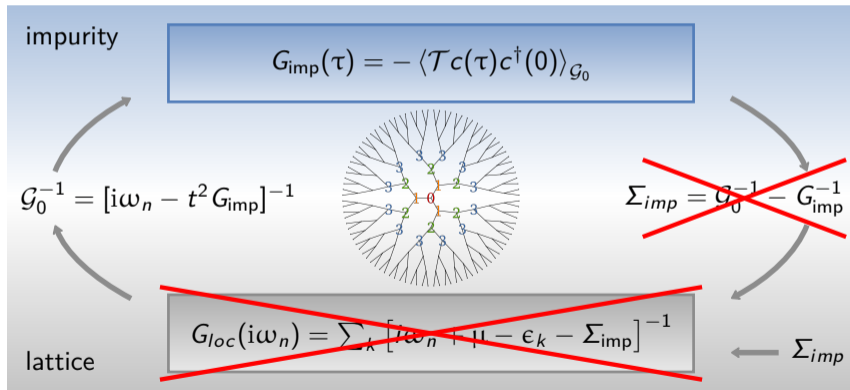
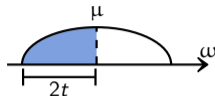
W. Metzner and D. Vollhardt, Phys. Rev. Lett. 62, 3 (1989)

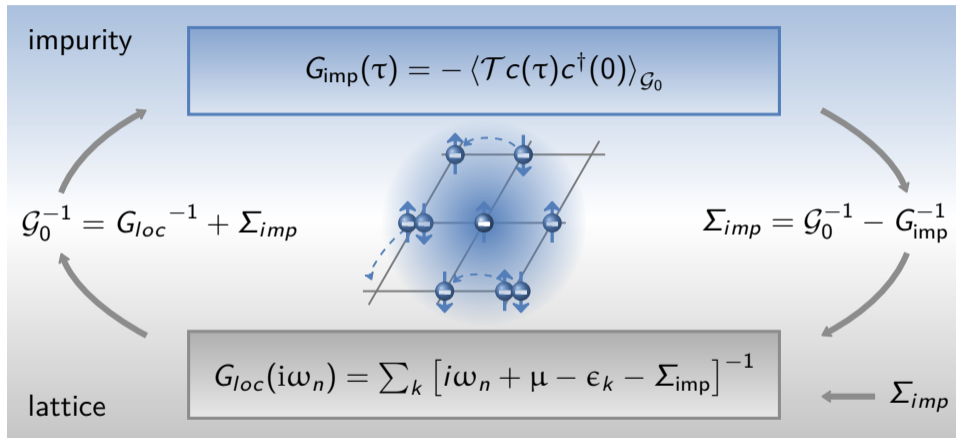
A. Georges and G. Kotliar, Phys. Rev. B 45, 12 (1992)

DMFT self-consistency - example: Bethe lattice

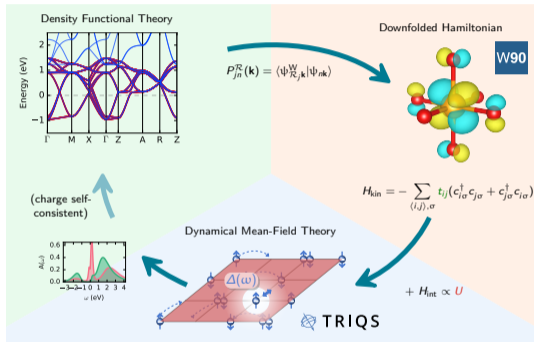
$z \rightarrow \infty$:

$$\rho(\omega) = \frac{1}{2\pi t^2} \sqrt{4t^2 - \omega^2}$$





- basic ingredients: t , U , and P



DFT+DMFT ingredients:

- target bands t
- projector functions P
- interaction Hamiltonian H_{int}
- (energy window, double counting, how to determine H_{int} , ...)
- impurity solver
- charge self-consistency
- ...

DFT+DMFT ingredients: target bands t

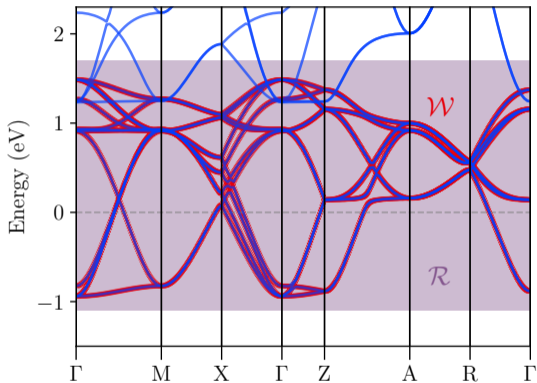
- partitioning of the system
- maximally localized Wannier functions $|\mathbf{R}j\rangle$ from Kohn-Sham states $|\psi_{n\mathbf{k}}\rangle$:

$$|\psi_{j\mathbf{k}}^{\mathbf{W}}\rangle = \sum_n V_{\mathbf{k},nj} |\psi_{n\mathbf{k}}\rangle$$

$$|\mathbf{R}j\rangle = \frac{V}{(2\pi)^3} \int_{\text{BZ}} d\mathbf{k} e^{-i\mathbf{k}\mathbf{R}} |\psi_{j\mathbf{k}}^{\mathbf{W}}\rangle$$

- hopping elements:

$$H_{\mathbf{k},ij}^{\mathbf{W}} = \langle \psi_{i\mathbf{k}}^{\mathbf{W}} | \hat{H} | \psi_{j\mathbf{k}}^{\mathbf{W}} \rangle \rightarrow t_{ij}(\mathbf{R}) = \langle \mathbf{0}i | \hat{H} | \mathbf{R}j \rangle$$



DFT+DMFT ingredients: projector functions P

lattice Green's function:

$$\hat{G}(\mathbf{k}, i\omega_n) = \left[(i\omega_n + \mu)\mathbb{1} - \hat{H}_{\mathbf{k}} - \Delta\hat{\Sigma}(\mathbf{k}, i\omega_n) \right]^{-1}$$

downfolding:

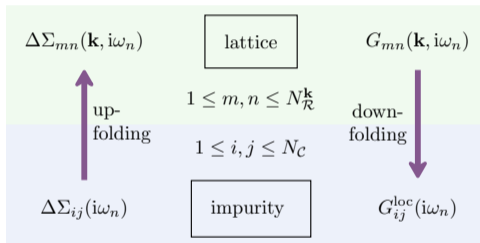
$$G_{ij,\mathcal{R}}^{\text{loc}}(i\omega_n) = \sum_{\mathbf{k}, mn} P_{im}^{\mathcal{R}}(\mathbf{k}) G_{mn}(\mathbf{k}, i\omega_n) P_{nj}^{\mathcal{R}*}(\mathbf{k})$$

with projector onto orbital j at atomic site \mathcal{R} :

$$P_{jn}^{\mathcal{R}}(\mathbf{k}) = \langle \psi_{\mathcal{R}j\mathbf{k}}^{\text{W}} | \psi_{n\mathbf{k}} \rangle$$

upfolding:

$$\Delta\Sigma_{mn}(\mathbf{k}, i\omega_n) = \sum_{\mathcal{R}, ij} P_{mi}^{\mathcal{R}*}(\mathbf{k}) \Delta\Sigma_{ij}^{\mathcal{R}}(i\omega_n) P_{jn}^{\mathcal{R}}(\mathbf{k})$$



- basis transformation
- entanglement
- local symmetries

Double counting

- E_U is a functional of the orbital occupations, but E_{XC} is a non-linear functional of the total electron density
- ill-posed problem due to the formally incompatible footing: diagrammatic vs. non-perturbative
- different analytic, *phenomenological* expressions have been proposed: FLL, AMF, ANI, Kunes, nominal...
- remedy: $GW+DMFT$

$$\Delta\Sigma_{ij}^{\mathcal{R}}(i\omega_n) = \Sigma_{ij}^{\mathcal{R}}(i\omega_n) - \Sigma_{DC}$$

$$E_{\text{DFT}+U}[\rho] = E_{\text{DFT}}[\rho] + E_U[n_{ij}^{\sigma}] - E_{\text{DC}}$$

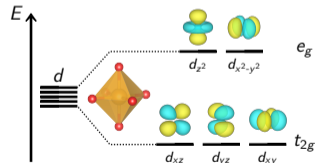
$$E_{\text{XC}} \approx E_{\text{XC}}^{\text{LDA}}[\rho] = \int d\mathbf{r} \epsilon_{\text{XC}}^{\text{hom}}[\rho(\mathbf{r})]\rho(\mathbf{r})$$

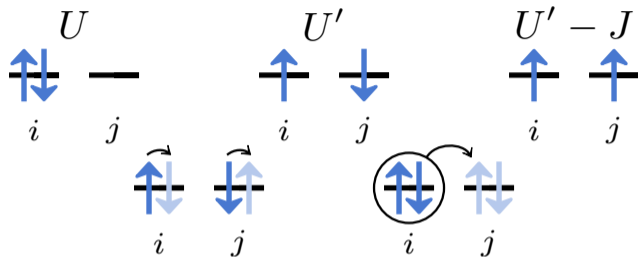
$$E_{\text{XC}}[n_{ij}^{\sigma}]?$$

$$\hat{H}_{\text{int}} = \frac{1}{2} \sum_{ijkl}^{\text{at } \mathcal{R}} U_{ijkl} c_i^\dagger c_j^\dagger c_l c_k$$

$$V_{ijkl} = \int d^3\mathbf{r} d^3\mathbf{r}' w_{i0}^*(\mathbf{r}) w_{j0}^*(\mathbf{r}') \frac{e^2}{|\mathbf{r} - \mathbf{r}'|} w_{l0}(\mathbf{r}') w_{k0}(\mathbf{r})$$

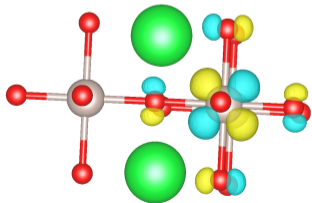
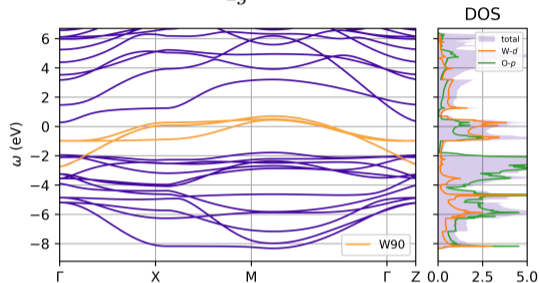
- complicated 4-rank tensor
- use symmetries to reduce complexity
- for cubic systems: Hubbard-Kanamori parametrization
- for spherical systems: Slater parametrization





$$\hat{H}_U = U \sum_i n_{i\uparrow} n_{i\downarrow} + U' \sum_{i \neq j} n_{i\uparrow} n_{j\downarrow} + (U' - J) \sum_{i < j, \sigma} n_{i\sigma} n_{j\sigma} - J \sum_{i \neq j} c_{i\uparrow}^\dagger c_{i\downarrow} c_{j\downarrow}^\dagger c_{j\uparrow} + J \sum_{i \neq j} c_{i\uparrow}^\dagger c_{i\downarrow}^\dagger c_{j\downarrow} c_{j\uparrow}$$

t_{2g} model



pros:

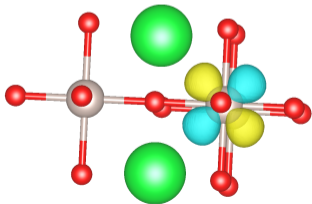
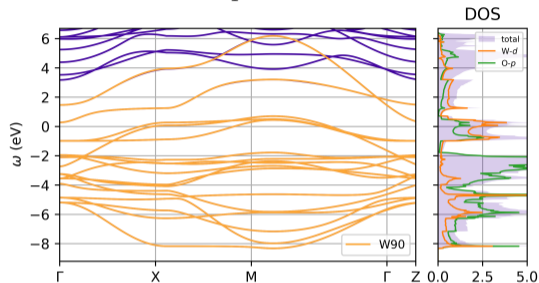
- no DC
- nominal occupations
- less work for impurity solver

cons:

- smaller U , more frequency-dependent
- larger spread Ω , oxygen tails \rightarrow less localized
- no information on e_g states...

DFT+DMFT ingredients: energy window

dp model



pros:

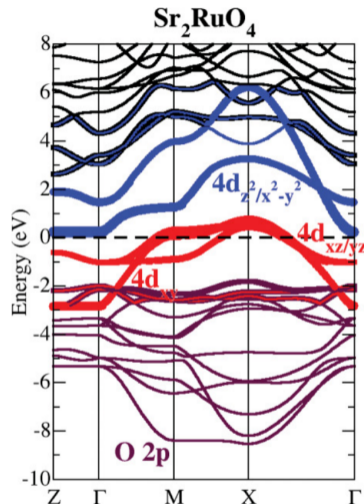
- more localized, DMFT more valid
- larger U and more atomic-like, less frequency-dependent
- renormalizes all states

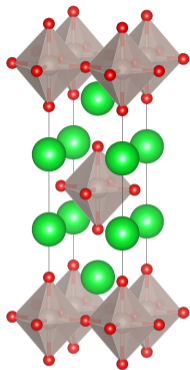
cons:

- DC, in principle U_{dp}, U_p
- fractional occupations
- heavy for impurity solver

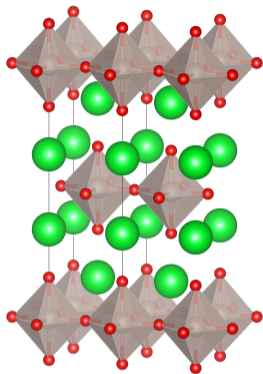
How to determine Coulomb interaction

- V of the order of 11 eV for t_{2g} ,
i.e. \gg bandwidth ≈ 3.4 eV
- effective Coulomb interaction screened by
surrounding electrons
- screened interaction $U(\mathbf{r}, \mathbf{r}')$ in practice:
 - cRPA: screening channels, frequency
dependence, Hund J
 - cLDA: only full d shell, static, no Hund J
- $d - dp$: $F^0 = 3.23$ eV, $\bar{U}_{mm} = 4.1$ eV,
 $t_{2g} - t_{2g}$: $\mathcal{U} = 2.56$ eV



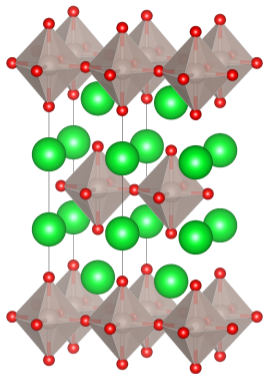


$$\Sigma = \left(\boxed{\Sigma_{\text{imp}}} \right)$$



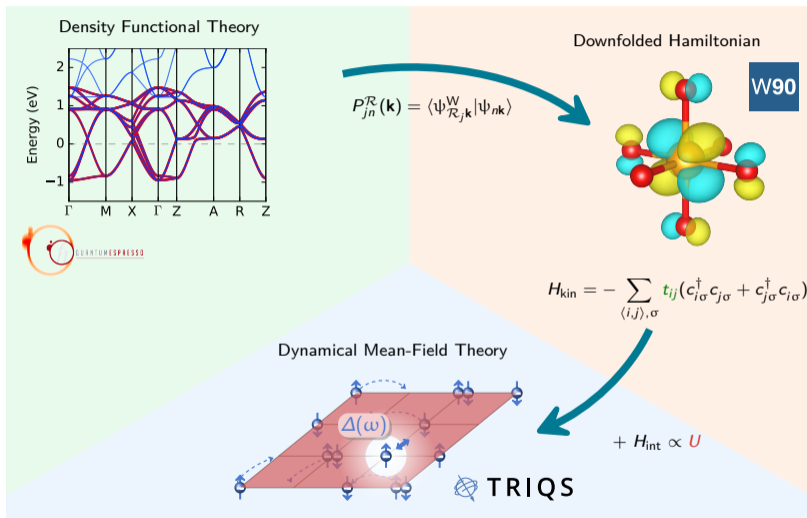
$$\Sigma = \begin{pmatrix} \Sigma_{\text{imp}}^1 & & & \\ & \Sigma_{\text{imp}}^2 & & \\ & & \Sigma_{\text{imp}}^3 & \\ & & & \Sigma_{\text{imp}}^4 \end{pmatrix}$$

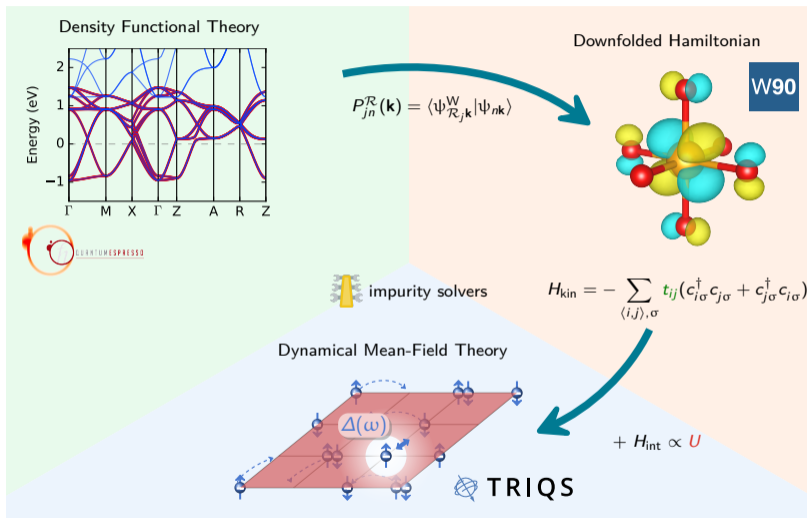
- self-energy approximated as block-diagonal in orbital basis

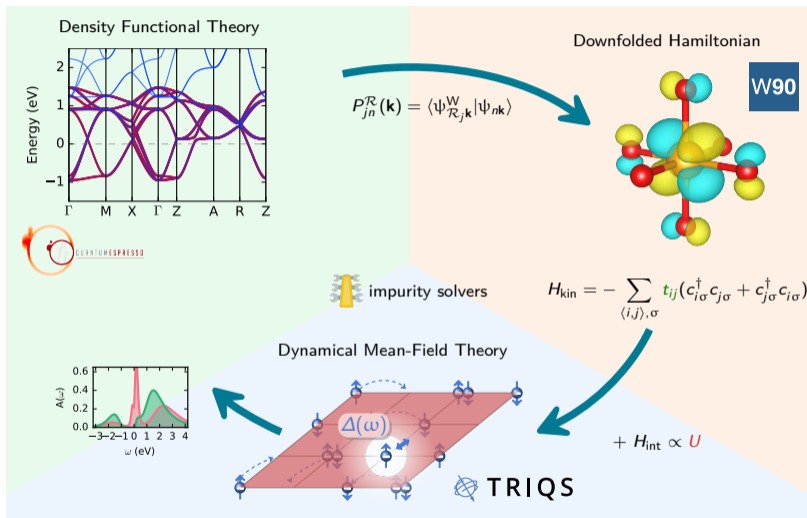


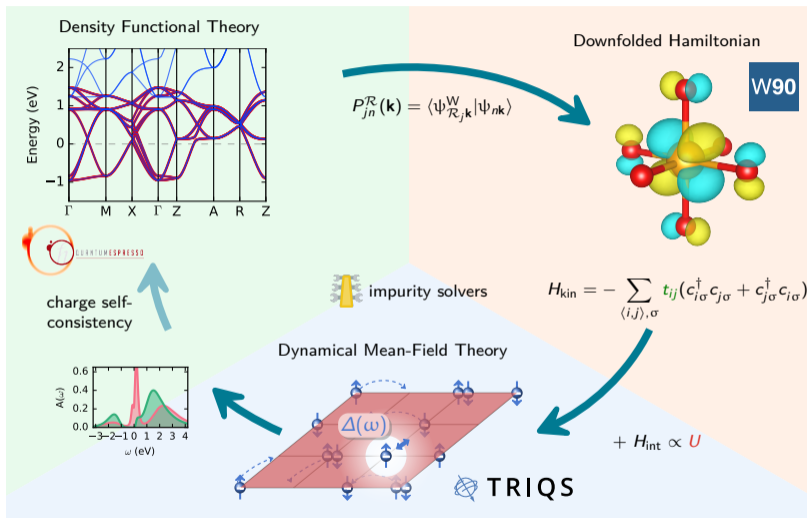
$$\Sigma = \left(\begin{array}{cccc} \Sigma_{\text{imp}}^1 & & & \\ & \square & & \\ & & \square & \\ & & & \square \end{array} \right)$$

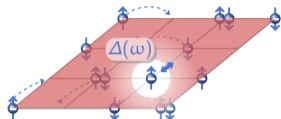
- self-energy approximated as block-diagonal in orbital basis
- map self-energy to symmetry-equivalent sites
- use spin channel for AFM solutions











$$G_{\sigma}^{\text{imp}}(\tau) = \langle \mathcal{T} c_{\sigma}(\tau) c_{\sigma}^{\dagger}(0) \rangle_{\mathcal{G}_0}$$



approximate solvers:

- Hartree(-Fock)
- Hubbard-I
- Iterated perturbation theory (IPT)
- Slave boson technique
- ...

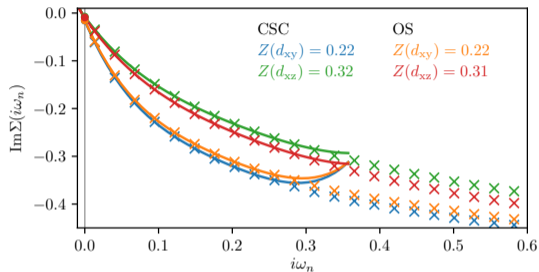
numerically exact solvers:

- Quantum Monte Carlo (QMC)
- exact diagonalization (ED)
- numerical renormalization group (NRG)
- density matrix renormalization group (DMRG)
- tensor-network based approaches (MPS/TTN)

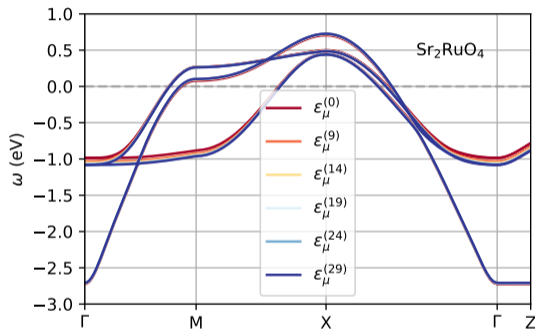
→ see other lectures in this school

Method	Physical quantity	Constraining field
Baym-Kadanoff	$G_{\alpha\beta}(\mathbf{k}, i\omega)$	$\Sigma_{\text{int},\alpha\beta}(\mathbf{k}, i\omega)$
DMFT (BL)	$G_{\text{loc},\alpha\beta}(i\omega)$	$\mathcal{M}_{\text{int},\alpha\beta}(i\omega)$
DMFT (AL)	$G_{\text{loc},\alpha\beta}(i\omega)$	$\Delta_{\alpha\beta}(i\omega)$
LDA+DMFT (BL)	$\rho(r), G_{\text{loc},ab}(i\omega)$	$V_{\text{int}}(r), \mathcal{M}_{\text{int},ab}(i\omega)$
LDA+DMFT (AL)	$\rho(r), G_{\text{loc},ab}(i\omega)$	$V_{\text{int}}(r), \Delta_{ab}(i\omega)$
LDA+ U	$\rho(r), n_{ab}$	$V_{\text{int}}(r), \lambda_{ab}$
LDA	$\rho(r)$	$V_{\text{int}}(r)$

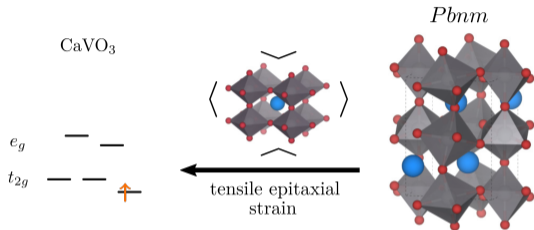
Quasiparticle mass renormalization in Sr_2RuO_4



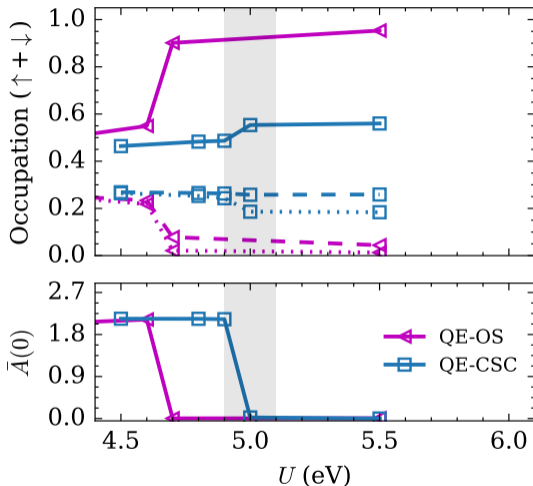
- CT-HYB solver, $\beta = 232 \text{ eV}^{-1}$
- minimal effect of charge self-consistency



Orbital polarization in CaVO_3 (tensile strain)

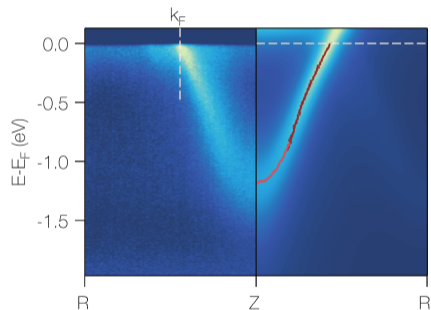


- CT-HYB solver, $\beta = 40 \text{ eV}^{-1}$
- charge self-consistency strongly reduces the orbital polarization found in one-shot calculations



What we can compute:

- spectral properties

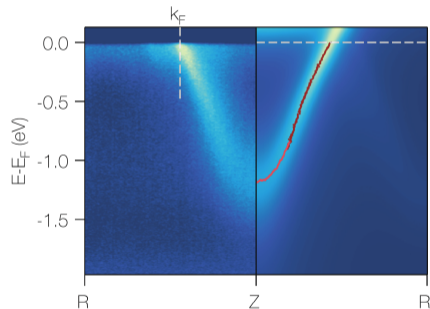


E. Cappelli *et al.*, *Phys. Rev. Mater.* 6, 075002 (2022)

A. Marrazzo, SB *et al.*, *arxiv:2312.10769* (2023)

What we can compute:

- spectral properties

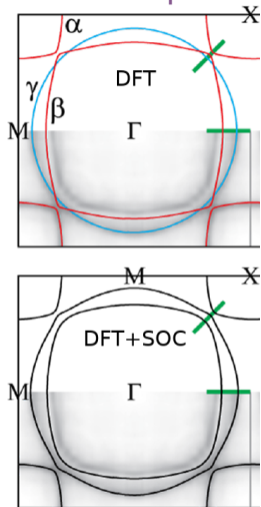


- optical and thermal conductivity
- Hall and Seebeck coefficient
- two-particle correlation function (susceptibilities)
- x-ray photoemission and absorption spectroscopy
- resonant inelastic x-ray scattering
- phonon spectra
- electronic Raman spectroscopy
- ...

E. Cappelli *et al.*, Phys. Rev. Mater. 6, 075002 (2022)

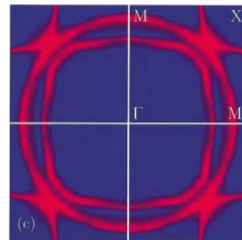
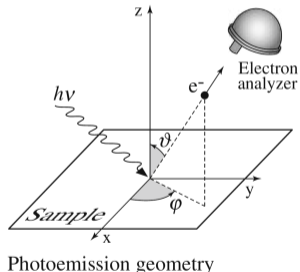
A. Marrazzo, SB *et al.*, arxiv:2312.10769 (2023)

Back to the experiment



$$E_{\text{kin}} = h\nu - \phi - |E_B|$$

$$\hbar\mathbf{k}_{\parallel} = \sqrt{2mE_{\text{kin}}} \cdot \sin \theta$$



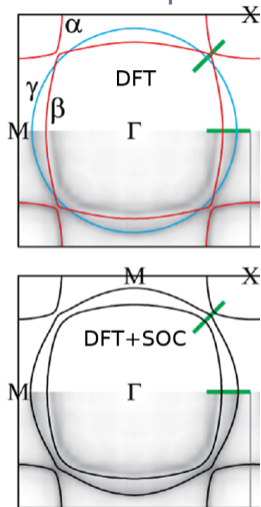
M. W. Haverkort *et al.*, Phys. Rev. Lett. 101, 026406 (2008)

A. Damascelli *et al.*, Rev. Mod. Phys. 75, 473 (2003)

A. Damascelli *et al.*, Phys. Rev. Lett. 85, 5194 (2000)

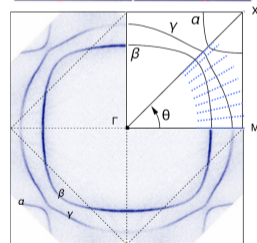
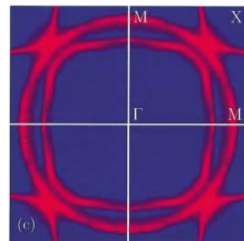
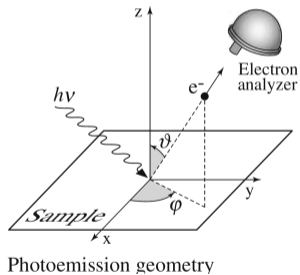
A. Tamai *et al.*, Phys. Rev. X 9, 021048 (2019)

Back to the experiment



$$E_{\text{kin}} = h\nu - \phi - |E_B|$$

$$\hbar\mathbf{k}_{\parallel} = \sqrt{2mE_{\text{kin}}} \cdot \sin \theta$$



M. W. Haverkort *et al.*, Phys. Rev. Lett. 101, 026406 (2008)

A. Damascelli *et al.*, Rev. Mod. Phys. 75, 473 (2003)

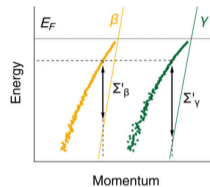
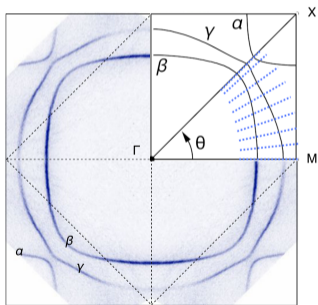
A. Damascelli *et al.*, Phys. Rev. Lett. 85, 5194 (2000)

A. Tamai *et al.*, Phys. Rev. X 9, 021048 (2019)

Is DMFT a good method for this application?

- QP equation:

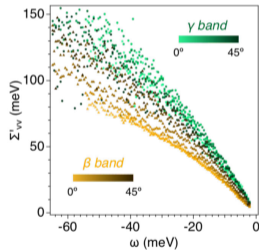
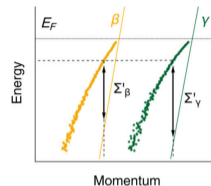
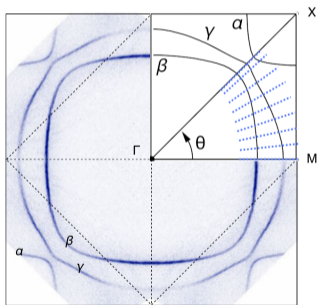
$$\omega - \epsilon_{\nu}(\mathbf{k}_{\max}^{\nu}(\omega)) - \Sigma'_{\nu\nu'}(\omega, \mathbf{k}_{\max}^{\nu}(\omega)) = 0$$



Is DMFT a good method for this application?

- QP equation:

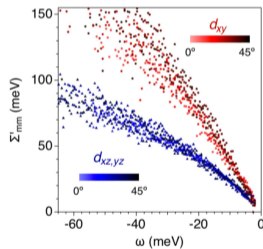
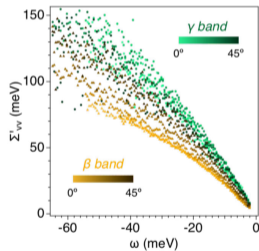
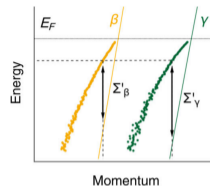
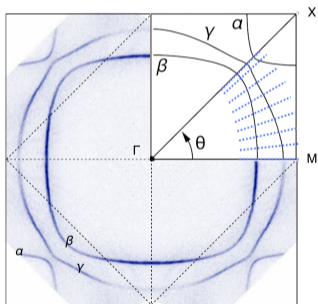
$$\omega - \epsilon_{\nu}(\mathbf{k}_{\max}^{\nu}(\omega)) - \Sigma'_{\nu\nu'}(\omega, \mathbf{k}_{\max}^{\nu}(\omega)) = 0$$



Is DMFT a good method for this application?

- QP equation:

$$\omega - \epsilon_{\nu}(\mathbf{k}_{\max}^{\nu}(\omega)) - \Sigma'_{\nu\nu'}(\omega, \mathbf{k}_{\max}^{\nu}(\omega)) = 0$$

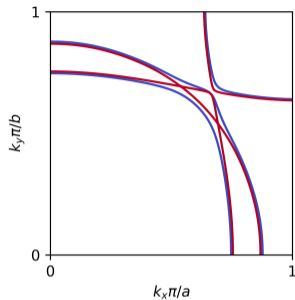
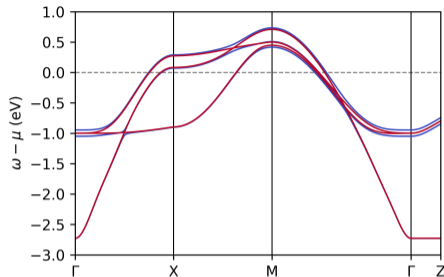


→ self-energy is local *in the orbital basis!*

Spin-orbit coupling in Sr_2RuO_4

spin-orbit coupling λ

$$c_{ij} = \begin{pmatrix} \epsilon_{xy} & 0 & 0 & 0 & \frac{\lambda_{xy}}{2} & \frac{i\lambda_{xy}}{2} \\ 0 & \epsilon_{yz} & -\frac{i\lambda_x}{2} & -\frac{\lambda_{xy}}{2} & 0 & 0 \\ 0 & \frac{i\lambda_x}{2} & \epsilon_{xz} & -\frac{i\lambda_{xy}}{2} & 0 & 0 \\ 0 & -\frac{\lambda_{xy}}{2} & \frac{i\lambda_{xy}}{2} & \epsilon_{xy} & 0 & 0 \\ \frac{\lambda_{xy}}{2} & 0 & 0 & 0 & \epsilon_{yz} & \frac{i\lambda_x}{2} \\ -\frac{i\lambda_{xy}}{2} & 0 & 0 & 0 & -\frac{i\lambda_x}{2} & \epsilon_{xz} \end{pmatrix}$$

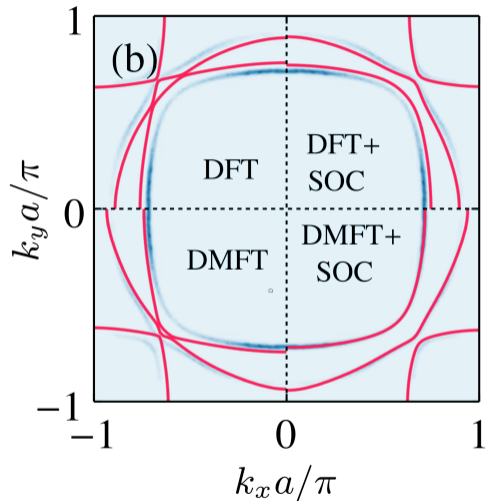


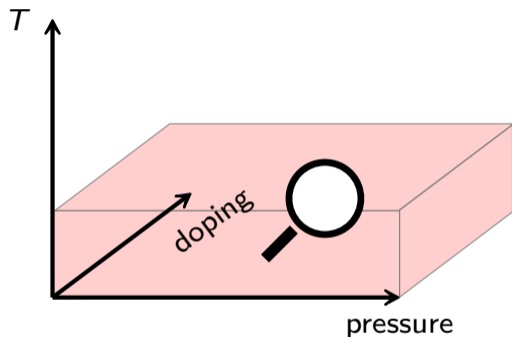
$$\hat{H}_\lambda^{\text{SOC}} = \frac{\lambda}{2} \sum_{ij} \sum_{\sigma\sigma'} c_{i\sigma}^\dagger (\mathbf{l}_{ij} \cdot \boldsymbol{\sigma}_{\sigma\sigma'}) c_{j\sigma'}$$

- correlation-induced enhancement of crystal-field splitting
- correlation-induced enhancement of effective spin-orbit coupling

Back to the experiment

- novel tree tensor-network impurity solver:
 - real-time/frequency axis
 - $T = 0$ K
 - energy-independent resolution
 - including spin-orbit coupling for the first time
- other quantities: mass enhancement, orbital occupations, optics, thermopower, Hall coefficient, magnetic susceptibility, RIXS, Raman scattering, ...





- double counting
- more orbitals, more complex systems
- screening
- (real-frequency) impurity solvers and analytic continuation
- superconductivity
- out of equilibrium
- low- T , exotic states